Electronic structure and superconductivity in strongly correlated systems in the pseudogap regime

L. Puig-Puig and F. López-Aguilar
Grup d'Electromagnetisme, Departament de Física, Edifici Cn, Universitat Autònoma de Barcelona, E-08193 Bellaterra (Barcelona), Spain
(Received 23 March 1995)

We propose effective potentials from a screened Coulomb interaction which arises from spin-fluctuation effects within a three-dimensional Hubbard single band model for systems with strongly correlated electrons within the pseudogap regime. This regime is characterized by the existence in the normal state of at least two structures located at both sides of the Fermi level and split by a gap or pseudogap. This is the most crucial assumption in the analysis performed in this work. We consider the proposed effective interactions between fermions, analyzing the possibility of obtaining superconductivity by means of the formulation of the corresponding Dyson-like equations for the normal and anomalous one-body propagators in the state with bosonic condensation. We also include vertex effects within these effective fermion-fermion interactions and discuss their influence in this formalism in order to consider a Migdal-like theory appropriate to Hubbard systems. In cases where superconductivity is found, the critical temperature is obtained and the influence of the band and potential parameters is analyzed.

I. INTRODUCTION

A relevant feature of the strongly correlated systems (SCS) is that the strong short-range interactions (SSRI's) and the hybridizations of localized states with others more extended cause a depletion in the density of quasiparticles near E_F leading to a pseudogap.[1,2] The spectral functions $A_{\mathbf{k}}(\omega)$ yield a density of quasiparticles, the pattern of which can be described by at least two peaks, one at each side of E_F.[1-3] The regime of these SCS with such $A_{\mathbf{k}}(\omega)$ is called pseudogap regime (PR).[2] The eventual increasing of the strength of the SSRI's can produce a true gap over the entire Fermi surface and then the system becomes an insulator, perhaps antiferromagnetic. The interest of the PR analysis is that the presence of this pseudogap is determinant in the appearance of instabilities. One of them can be superconductivity, the properties of which (superconducting gap, transition temperature, pairing potential, etc.) are quantitatively dependent on the density of states (DOS) near E_F. The charge and spin fluctuations are SSRI's which govern the PR state and these fluctuations are strongly dependent on the occupation ratio of the localized states, with respect to the extended ones. This ratio is crucial for the appearance of superconductivity in both heavy-fermion systems and doped (molecular and high-T_c) superconductors. Therefore, the charge and spin fluctuations can be considered as the starting point for obtaining a mechanism for superconductivity in systems with strongly correlated electrons.[4,5] These fluctuations originate interfermionic coupling potentials, the features of which may be compatible (or not) with the existence of bosonic condensation and superconductivity, depending on the band parameters of the electronic structures of these strongly correlated systems. It is still not clear which effective potentials are able to give rise to these kinds of superconductivity when introduced into the strong-coupling superconductivity equations. In the present paper, we deal with the effective interaction between fermions with antiparallel spins. The study is performed considering an appropriate scheme for a generic strongly correlated system in the pseudogap regime.[1-3] In this regime, the partial DOS of each strongly correlated orbital in the interacting system without pairing and superconductivity can be simulated by two Lorentzians, at least, one at each side of E_F, split by 2λ and with half widths Λ. The pattern of this PR electronic structure can be seen in previous literature.[1-3,6] This DOS is used to determine a susceptibility response function and the corresponding fermion-fermion interactions which produce the pairing potential. This pairing potential is obtained by means of the well known Berk-Schrieffer theory for the spin fluctuation exchange.[7-9] We also analyze the conditions of the band parameters for obtaining a Migdal-like theorem in the case of a fermion-fermion interaction arising from the "Hubbard U" in SCS in PR. We introduce the resulting fermion-fermion interaction into the Dyson equations appropriate to the case with bosonic condensation, in order to elucidate which band parameters describing the electronic structure are more favorable to yield superconductivity. In recent works, some authors[4] have solved similar equations without taking into account vertex effects and considering two-dimensional Hubbard systems with a tight-binding band and within the half-filling condition. The use of the half filling of the band and its tight-binding dispersion energy is justified in two-dimensional systems, among other reasons, because of the high complexity and difficulty of the calculations without considering these conditions; however, both conditions are not

clearly compatible with all strongly correlated electronic structures, especially in SCS in PR (for instance, in intermediate valence, heavy-fermion systems, and molecular crystals). The model for the susceptibility response function $\chi(\omega)$ and the consideration of vertex effects is what makes our analysis fundamentally different from that of Ref. 4. Vertex effects can be important and even decisive in the pairing potentials for some band parameter values (narrow bandwidths and large U). The $\chi(\omega)$ proposed in our work is obtained from a DOS which is valid for some three-dimensional Hubbard systems that present the PR features and, in addition, our model does not require the half-filling condition, although this condition facilitates the calculations.

In short, the aim of this paper is to analyze the relation between the electronic structure and the superconductivity of the strongly correlated systems considering short-range interactions and an isotropic form for the superconducting gap. In addition, we exploit the characteristics of the DOS of the strongly correlated systems in the pseudogap regime. The scheme of the fermion-fermion interaction is considered within the Berk-Schrieffer-like theories of the spin fluctuations, and we solve the Dyson equation at finite temperature within the boson condensation state. In Sec. II, we analyze the different interactions with and without vertex effects. In Sec. III, we calculate the full nondiagonal Green's function in the superconducting state, and we also analyze the evolution of the transition temperature as a function of the several band parameters. In Sec. IV, we summarize the conclusions.

II. EFFECTIVE FERMION-FERMION INTERACTION

To study the effective interaction between fermions with antiparallel spins, we consider the Berk-Schrieffer theory,[7–9] which takes into account the diagrams corresponding to the subset of the random-phase approximation (RPA) series with an odd number of U interactions, and also the diagrams of the electron-hole ladder approximation (EHLA) [see Fig. 1(b)]. These interactions correspond to spin fluctuations.[7–9] The reason for formulating the perturbative treatment from these two series is that both series, RPA and EHLA, are nonredundant and complementary in the sense that the former is dominant in systems with a large number of interacting particles,

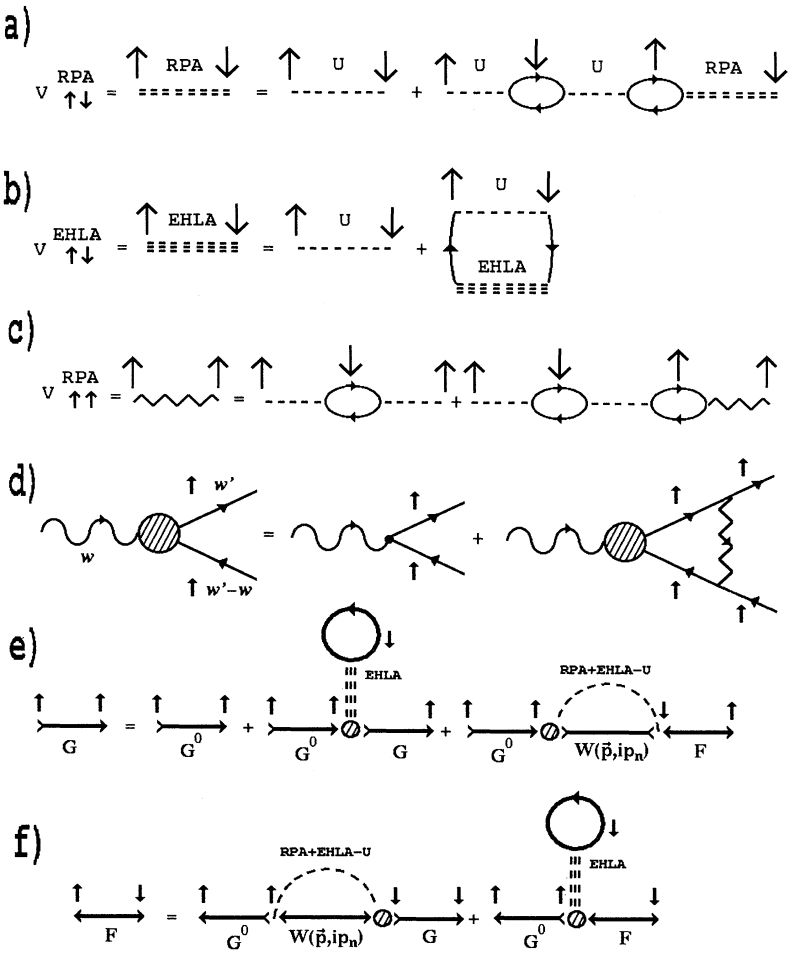

FIG. 1. Feynman diagrams corresponding to (a) effective interaction between fermions with antiparallel spins from the corresponding subset of the RPA series; (b) effective interaction between antiparallel spins obtained from the EHLA series; (c) RPA effective interaction between fermions with parallel spins; (d) recurrent vertex equation; (e) and (f) Dyson-like equations for the normal and anomalous Green's functions.

while the latter is significative for a small number.

These two effective interactions (see Fig. 1), are given by

$$V_{\uparrow\downarrow}^{\mathrm{RPA}}(\omega_t) = \frac{U}{1 - U^2\chi^2(\omega_t)}, \tag{1}$$

$$V_{\uparrow\downarrow}^{\mathrm{EHLA}}(\omega_d) = \frac{U}{1 + U\chi(\omega_d)}, \tag{2}$$

$$V_{\uparrow\downarrow}^{\mathrm{RPA+EHLA}}(\omega_t, \omega_d) = \frac{U}{1 - U^2\chi^2(\omega_t)} + \frac{U}{1 + U\chi(\omega_d)} - U, \tag{3}$$

where $\chi(\omega)$ is a linear susceptibility response, which is crucial in the determination of the effective potentials and self-energies, ω_t stands for the frequency transferred by the interaction, and ω_d corresponds to the difference of the frequency of the outcoming particle 2 and that of the incoming particle 1. The term $-U$ appears in Eq. (3) in order to avoid redundances when summing both series RPA and EHLA. The $\mathbf{q}$ dependence is dropped by averaging over the first Brillouin zone. This local approximation has always been justified in Hubbard systems by the localization of the strongly correlated electrons[10] since, in these systems, it is commonly accepted that the effective interactions arising from the U energy depend slowly on the quasimomentum when one considers an electronic structure where the localization effects are implemented[10,11] in the calculation of screening. Of course, the local approximations of the effective interaction and self-energies are more compatible in the tridimensional Hubbard systems than in the 2D ones. The general expression for this $\mathbf{q}$ averaged $\chi(\omega)$ is given by

$$\chi(\omega) = \sum_m \int_{-\infty}^{0} dx \int_0^{\infty} dx' N_m(x) N_m(x') \times \left[\frac{1}{\omega + x - x' + i0^+} - \frac{1}{\omega + x' - x - i0^+} \right]. \tag{4}$$

As we have said above, in a generic SCS in PR, the interacting-system DOS is given by

$$N(\omega) = \sum_m \left(\frac{A_m \Lambda_m}{(\omega + \lambda_m)^2 + \Lambda_m^2} + \frac{B_m \Lambda'_m}{(\omega - \lambda'_m)^2 + \Lambda_m'^2} \right), \tag{5}$$

where the index m runs over the strongly correlated orbital symmetries, A_m and B_m are the weight of the corresponding Lorentzian curve, λ_m (λ'_m) is the energy of the resonance located below (above) E_F, and Λ_m and Λ'_m are the corresponding widths of these resonances. Then the susceptibility response $\chi(\omega)$ of expression (4) can be written as[3]

$$\chi(\omega) = \sum_m \left[\frac{\alpha_m}{\omega - \gamma_m + i\Gamma_m} + \frac{\alpha_m}{-\omega - \gamma_m + i\Gamma_m} \right], \tag{6}$$

where α_m, γ_m, and Γ_m are parameters that depend on A_m, B_m, λ_m, λ'_m, Λ_m, and Λ'_m. When the splitting between the two Lorentzian curves is large enough so that their overlap is small, the parameters α_m, γ_m, and Γ_m in (6) have the meaning of $\alpha_m \equiv n_m(1 - n_m)$ (where n_m is the occupation of the m orbital symmetry), $\gamma_m \equiv \lambda_m + \lambda'_m$ (the splitting between the two Lorentzian curves of the m symmetry DOS of the strongly correlated orbital), and $\Gamma_m \equiv \Lambda_m + \Lambda'_m$ (the sum of their two half widths).

In Fig. 2, we compare the results of $\chi(\omega)$ obtained from Eq. (6) with the numerical result of the integral (4), for a DOS constituted by a double-Lorentzian characterized by the parameters λ and Λ. In this figure, we can see that the evolution with these band parameters is similar in both cases, although there are quantitative differences, especially when $\lambda \sim \Lambda$. Therefore, this figure allows us to conclude that the expression (4) should be used in the cases in which $\lambda \sim \Lambda$, and (6) may be used in cases in which $\lambda >> \Lambda$. However, we note the qualitative similarity of the their evolutions in both cases.

The effective interaction (3) can be written in the case of double Lorentzian DOS, in terms of the band parameters:

$$V_{\uparrow\downarrow}^{\mathrm{RPA+EHLA}}(\omega_t, \omega_d) = U + U \left(\frac{f_1}{\omega_t^2 - \Omega_1^2} + \frac{f_2}{\omega_d^2 - \Omega_2^2} \right), \tag{7}$$

where the strengths of the oscillators are of opposite sign and with values equal to

$$f_1 = (\Omega_1^2 - y^2)/2$$

and

$$f_2 = -3f_1, \tag{8}$$

and

$$y^2 = \beta^2 = (\gamma - i\Gamma)^2 , \tag{9}$$

$$\Omega_1^2 = \beta^2 + 2\alpha U\beta , \tag{10}$$

$$\Omega_2^2 = \beta^2 - 2\alpha U\beta = 2y^2 - \Omega_1^2 , \tag{11}$$

where α, γ, and Γ are defined in expression (6). Expression (7) can be understood as the sum of a repulsive interaction U, plus two oscillators with a strength given by the corresponding numerator, and each oscillator can be physically interpreted as a fermion-fermion interaction produced by an intermediating boson characterized by the corresponding pole Ω_k. Each oscillator intervenes in the time-dependent effective interaction as a damped oscillating function, the frequency of which is the real part of Ω_k and the damping constant of which is the imaginary part of Ω_k. This picture arising from the potential (7) appears in a similar way in other theories with intermediating bosons, which can present the pair potential as sum of two oscillators, each one with its own frequency.[12] The main parameters which intervene in the boson condensation are the strength of the oscillator, the value of the oscillation frequencies, and the damping constant, which is described by the imaginary part of these

extended frequencies. The poles Ω_1 and Ω_2 of (7), and y, depend on the band parameters λ and Λ in such a way that when we give a fixed value for these parameters, all the Ω poles are, then, determined by means of expressions (9)–(11). However, we will consider Ω_1, Ω_2, and y as independent parameters from λ and Λ, thus extending the study to regions of the band-parameter space, which are out of those that would correspond to the spin-fluctuation theory used for determining the potential (7). At this point the vertex effects can be decisive since, due to their capability for producing instabilities, we can obtain vertex-containing pair potentials, the effects of which can quantitatively enhance the boson condensation and even induce superconductivity in some cases where the potential (7) is unable.

When introducing the potential (7) into the $W(\omega)$ self-energy equation (see Sec. III), it appears there as

$$V_{\uparrow\downarrow}^{\mathrm{RPA+EHLA}}(\omega_t,\omega_d) = V_{\uparrow\downarrow}^{\mathrm{RPA}}(\omega_t) + V_{\uparrow\downarrow}^{\mathrm{EHLA}}(\omega_d) - U \ , \tag{12}$$

where ω_d and ω_t have been defined below (3). Because of frequency conservation in the vertices, in this case $\omega_d = \omega_t + 2\omega$, where the frequency ω is that corresponding to the self-energy, and ω_t is the integration variable ω' when one calculates W [see below, Eqs. (16), (17), and (19)]. The curve shown in Fig. 3 (dotted line) represents the potential (12) as a function of ω_t for $\omega = 0$. In this case, the region where the real part is negative is larger than in the full RPA effective interaction and reaches the origin, resembling, therefore, the typical shape used in BCS-like theories. For large frequencies, the screening disappears and the interaction tends to the bare U. This behavior is roughly maintained, while ω is not too large.

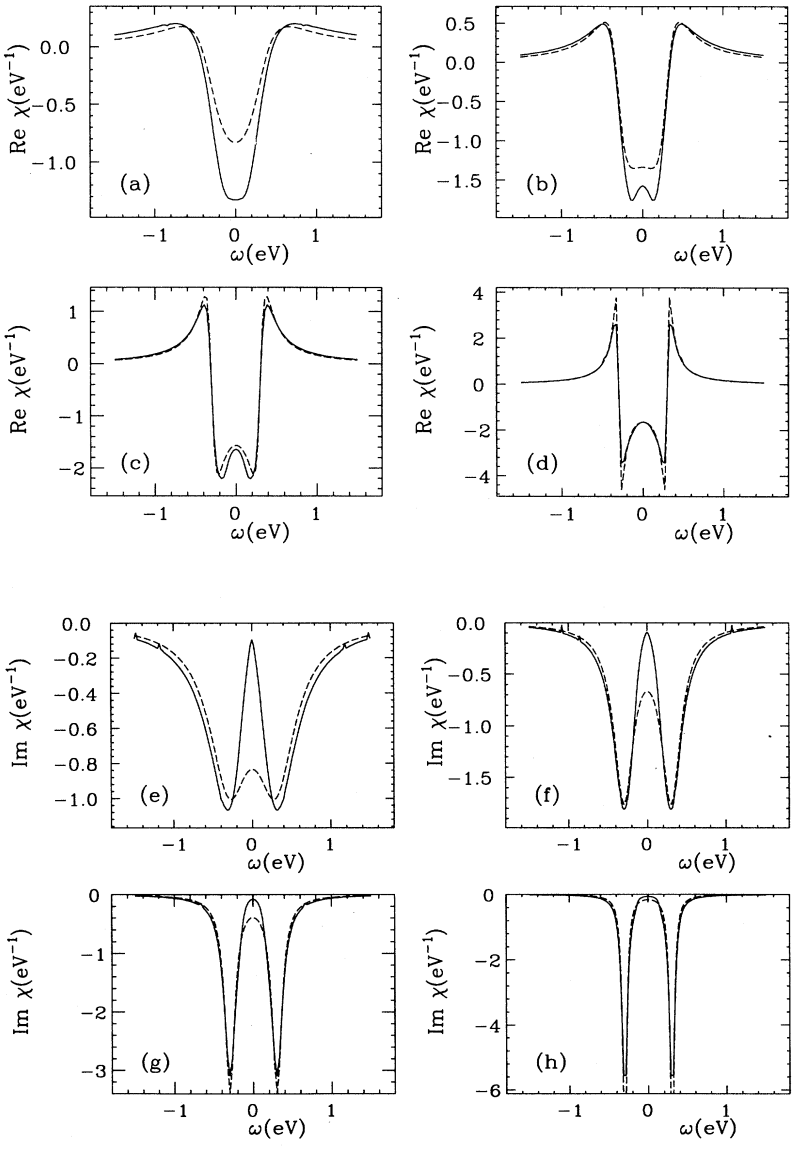

FIG. 2. (a)–(d): real part of $\chi(\omega)$ calculated with expressions (4) (solid line) and (6) (dashed line) for different values of the ratio between λ and Λ: (a) $\lambda = \Lambda$, (b) $\lambda = 2\Lambda$, (c) $\lambda = 4\Lambda$, and (d) $\lambda = 10\Lambda$. (e)–(h): the corresponding imaginary part. In all cases λ=0.15 eV and $n = 0.5$.

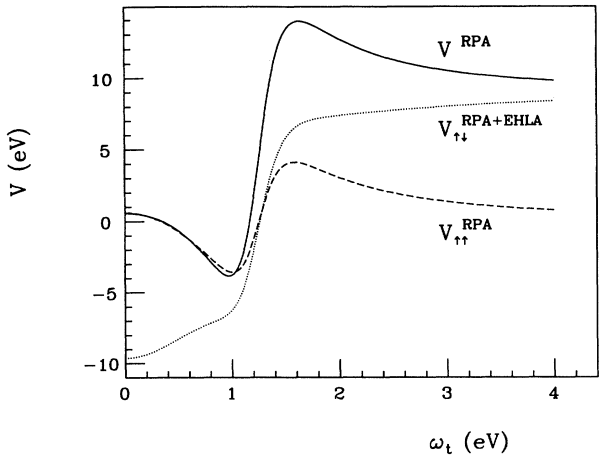

FIG. 3. Solid line: real part of the effective potential from the full RPA series; dashed line: RPA effective interaction between parallel spins; dotted line: RPA+EHLA interaction between antiparallel spins as a function of ω_t with $\omega = 0$; see below Eq. (12).

Effective fermion-fermion interaction with vertex effects

The exclusion of the vertex effects in the effective interaction in superconductors with mediating phonons is justified, because of the large mass of the ions, with respect to the electrons, so that the influence of these Feynman diagrams is small, due to the weak phonon-electron coupling. This assertion constitutes the Migdal theorem,[13] which has been sufficiently proved in phonon-mediated superconductors. However, when the effective pair coupling interaction comes from the Hubbard U, this theorem has not been established and many authors claim that vertex effects should be included in the effective fermion-fermion interaction, both in the Eliashberg-like equations and in the calculation of the screened Coulomb interaction,[4,11] above all if one considers that these vertex effects can origin instabilities. The dressed vertex in the local interaction approximation considered in this paper satisfies the equation [see Fig. 1(d)]

$$\gamma_{\uparrow\uparrow}(\omega,\omega') = 1 + \frac{i}{2\pi}\int_{-\infty}^{\infty}\sum_{\mathbf{q'p}} G_{\mathbf{q'}}(\omega'')G_{\mathbf{q'-p}}(\omega''-\omega) \times V_{\uparrow\uparrow}^{\mathrm{RPA}}(\omega''-\omega')\gamma_{\uparrow\uparrow}(\omega,\omega'')d\omega'' , \quad (13)$$

where $V_{\uparrow\uparrow}^{\mathrm{RPA}}(\omega)$ is the RPA potential with an odd number of electron-hole RPA loops and the analytic expression of which can be deduced from [see Fig. 1(c)]

$$V_{\uparrow\uparrow}^{\mathrm{RPA}}(\omega) = \frac{U^2\chi(\omega)}{1-U^2\chi(\omega)^2}. \quad (14)$$

This interaction, considering the susceptibility (6), can be expressed as

$$V_{\uparrow\uparrow}^{\mathrm{RPA}}(\omega) = U\left(\frac{f_1}{\omega^2-\Omega_1^2}+\frac{f_1}{\omega^2-\Omega_2^2}\right), \quad (15)$$

being f_1, Ω_1, Ω_2, and y, those of expressions (8)–(11). The Green's functions which appear in (13) correspond to the interacting system. They are self-consistently calculated in the following section, by means of the so-called Eliashberg equations. The first step for the calculation of (13) is to perform the double sum $\sum_{\mathbf{pq'}} G_{\mathbf{q'}}(\omega'')G_{\mathbf{q'-p}}(\omega''-\omega)$, which is obtained from the interacting-system DOS coming from the full Green's function [i.e., $N_s(\omega) = \frac{1}{\pi}\sum_{\mathbf{k}}|\mathrm{Im}G_{\mathbf{k}}(\omega)|$].

The γ equation is solved self-consistently, and the results for the first iteration and the self-consistent solution (given in the real axis) are shown in Fig. 4. From inspection of this figure, we can deduce that this vertex function is symmetric versus ω', has variations in an interval $|\omega'| \leq 10$ eV, and tends to 1 (vanishing vertex effects) for large ω'. In addition, we can see in this figure that the self-consistent solution differs from the first iteration when the splitting between the two resonances at both sides of E_F and the width of these resonances are narrow.

The effective interaction considering vertex effects which has to be included in the Dyson equation for obtaining the anomalous self-energy, can be written as

$$V_{\mathrm{eff}}^{(\gamma)}(\omega,\omega') = \left[V_{\uparrow\downarrow}^{\mathrm{RPA}}(\omega') + V_{\uparrow\downarrow}^{\mathrm{EHLA}}(2\omega+\omega') - U\right]\gamma_{\uparrow\uparrow}(\omega',\omega+\omega'). \quad (16)$$

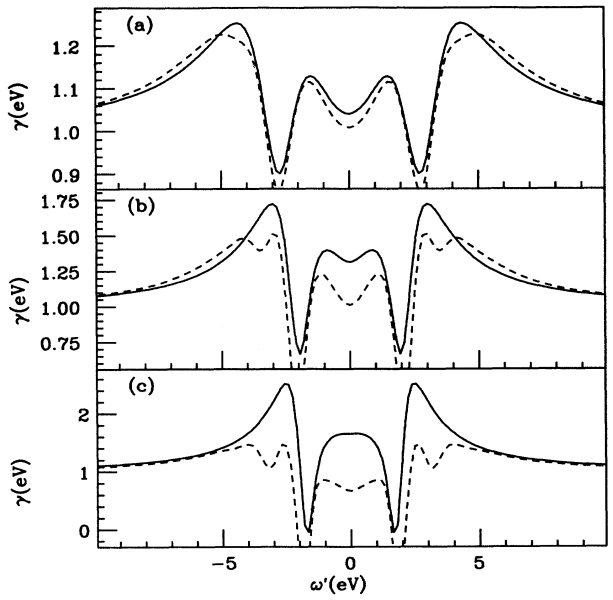

FIG. 4. Vertex function, see Eq. (13), with $\omega = 0$ for different values of λ and Λ. Solid lines correspond to the first iteration vertex function and dashed lines represent the self-consistent solutions. (a) for λ =1.5 eV and Λ =1 eV; (b) for λ =0.75 eV and Λ =0.50 eV; (c) for λ =0.50 eV and Λ =0.25 eV.

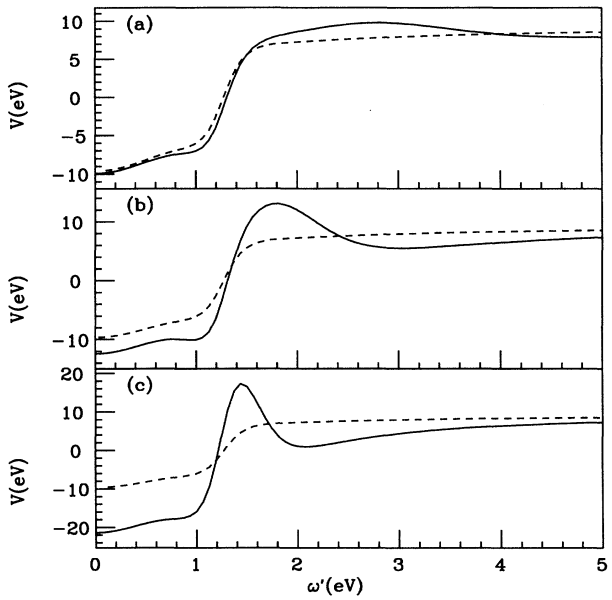

FIG. 5. Effective potential with and without vertex effects corresponding to Eqs. (16) and (12), respectively, for different values of λ and Λ. Solid lines correspond to potentials with vertex effects and dashed lines to potentials without vertex effects. (a) λ =1.5 eV and Λ =1 eV; (b) λ =0.75 eV and Λ =0.50 eV; (c) λ =0.50 eV and Λ =0.25 eV. In all cases, $\omega = 0$.

In Fig. 5, we represent the effective interaction with and without vertex effects. Both potentials are drawn for $\omega = 0$, and one can see that the pair potentials with these effects present a deeper negative region. They also present sharper variations in the repulsive zone. In addition, it is important to note that the differences between the corresponding pair potentials, with and without γ function, are smaller for increasing splitting and bandwidths of the characteristic PR resonances, being vertex effects irrelevant (i.e., $\gamma_{\uparrow\uparrow} \simeq 1$) for values of $\lambda \geq 1.5$ eV.

III. ELIASHBERG EQUATIONS

Given the existence of a large region where the potential is attractive,[14] one expects it can originate superconductivity. To check this possibility, we have developed the corresponding anomalous and normal self-energy equations considering the potential (16) and we have obtained

$$W(\omega) = \int_{-\infty}^{\infty} d\omega' K_W(\omega,\omega') \times \mathrm{Im}\int_{-\infty}^{\infty} \frac{-N(x)W(\omega')}{\omega'^2 Z(\omega')^2 - x^2 - W(\omega')^2} dx \ , \quad (17)$$

$$S(\omega) = -\int_{-\infty}^{\infty} d\omega' K_S(\omega,\omega') \times \mathrm{Im}\int_{-\infty}^{\infty} \frac{N(x)\,[\omega' Z(\omega') + x]}{\omega'^2 Z(\omega')^2 - x^2 - W(\omega')^2} dx, \quad (18)$$

where $N(\omega)$ is the DOS of the interacting, nonsuperconducting state, which is fitted by an expression of the type (5), and $K_W(\omega,\omega')$ and $K_S(\omega,\omega')$ have the following expressions:

$$K_W(\omega,\omega') = -\frac{1}{\pi}\sum_k \mathrm{Res}[V_{\mathrm{eff}}^{(\gamma)}(\omega,\Omega_k)]\frac{n_B(\Omega_k)}{\omega+\Omega_k-\omega'} + V_{\mathrm{eff}}^{(\gamma)}(\omega,\omega')n_F(\omega') \ , \quad (19)$$

$$K_S(\omega,\omega') = -\frac{1}{\pi}\gamma_{\uparrow\uparrow}(0,\omega) \times\left(\sum_k \mathrm{Res}[V_{\uparrow\downarrow}^{\mathrm{EHLA}}(\Omega_k)]\frac{n_B(\Omega_k)}{\omega+\Omega_k-\omega'} - V_{\uparrow\downarrow}^{\mathrm{EHLA}}(\omega'-\omega)n_F(\omega')\right). \quad (20)$$

It should be noted that in Eq. (19), Ω_k are the poles of both the potential (7) and the γ function. Although the two potential poles (Ω_1 and Ω_2) and y depend on the band parameters (λ, Λ, and U), we have considered them as independent in order to study separately their influence on the band-parameter space superconducting region.

As a first step we have solved self-consistently Eqs. (17) and (18) using potential (7), i.e., without considering vertex effects. The solution is different from zero for some of the band parameters. The range of λ and Λ values for which a nonzero convergent solution can be obtained is large: it ranges from about 1.5 eV to more than 3 eV and from $\simeq$1 eV to also high values, respectively. We note that in this region, vertex effects are small: $\gamma \simeq 1$. The superconducting solution of (17) and (18) found in this region of the λ-Λ space is obtained with values of the potential parameters Ω_1, Ω_2, and y, which are different from those arising from expressions (9)–(11). The values of λ and Λ compatible with the employed potential parameters according to these expressions should be $\simeq$ 0.15 eV. This implies that the potential (7) can yield superconductivity, but only if one of its poles has a lower value than the given by expressions (9)–(11). This discrepancy may be interpreted by considering that the spin fluctuation arising from the potential (7) is, in this case, unable to by itself obtain superconductivity and it requires either the aid of another lower energy oscillator or a more complex pairing potential. The convergent solutions for the gap $\Delta(\omega) = W(\omega)/Z(\omega)$, which result in this case from the self-energy equations, are represented in Fig. 6 for various values of the real part of the pole Ω_1 [as defined in expresion (7)]. The shape of the curves is as expected for a superconducting gap function[15] and similar to other cases, as those analyzed by Monthoux and Scalapino in Ref. 4: it is positive up to a given frequency where there is an oscillation and for larger frequencies the gap is negative, tending to a constant and negative value. Although it is usual to find several peaks in the gap $\Delta(\omega)$, we obtain only one, because our pairing potential is simplified and has only two poles with only one of them causing oscillations in the potential.

In a second step, we have solved Eqs. (17) and (18) in

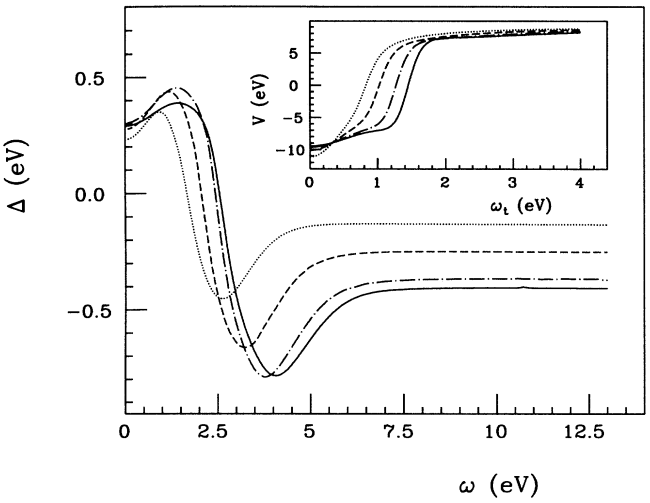

FIG. 6. Superconducting gap obtained from the Eliashberg equations without vertex effects for different values of the potential parameter $\mathrm{Re}\Omega_1$. Solid line: $\mathrm{Re}\Omega_1$=1.43 eV; dot-dashed line: $\mathrm{Re}\Omega_1$=1.25 eV; dashed line: $\mathrm{Re}\Omega_1$=1.00 eV; dotted line: $\mathrm{Re}\Omega_1$=0.80 eV. Inset: $V_{\uparrow\downarrow}^{\mathrm{RPA+EHLA}}$ as a function of ω_t (with $\omega = 0$) corresponding to the same parameter values. In all cases, $\mathrm{Im}\Omega_1$=-0.31 eV, $y = 0.3 - 0.15i$ eV, $U = 9$ eV, $\lambda = 2$ eV, and $\Lambda = 2$ eV.

the region where vertex effects have an important contribution, that is, for smaller values of λ and Λ. We have found convergent solutions, which present a structure with several peaks due to the bigger complexity of the potential with vertex effects (see Fig. 7). It should be remarked that these solutions are obtained with values of λ and Λ compatible with those of the poles according to (9)–(11) and, as said above, this means that the spin fluctuations with vertex effects could be sufficient for obtaining susperconductivity in strongly correlated systems. The density of states of the superconducting state can be directly obtained from expression (5) and the convergent solutions of $W(\omega)$, by means of the following expression:

$$N_s(\omega) = \frac{1}{\pi}\sum_{\mathbf{k}} |\mathrm{Im}G_{\mathbf{k}}(\omega)| \simeq \left|\mathrm{Re}\frac{N(\omega)\omega}{\sqrt{\omega^2 - \Delta^2(\omega)}}\right|. \quad (21)$$

For the cases as that in Fig. 7 (i.e., with vertex effects), it presents a complex pattern, with more peaks than that corresponding to the gap of Fig. 6 (i.e., without vertex effects). However, in both cases the optical superconducting gap Δ_0 defined by $\Delta_0 = \Delta(\omega = \Delta_0)$ presents similar values.

The PR features of the renormalized DOS are, obviously, reinforced in the superconducting state due to the appearance of the superconducting gap, since this enhances the splitting between the structures near to E_F. As a consequence, the conditions for implementing the PR model are ensured and one can fit $N_s(\omega)$ by means of analytical expressions of the type (5). Thus, the calculations of the γ and $W(\omega)$ functions [Eqs. (13) and (17)] of the superconducting state are facilitated. Besides, taking into account the different energy scale of the superconducting gap and the splitting between the lower and upper Hubbard bands,[3] only the structures close to E_F have decisive influence in the Eliashberg equations. However, it should be noted that the decrease of the number of states near to E_F, due to existence of a nonzero solution for $W(\omega)$, is in detriment of the appearance of the superconductivity. This is why the relaxation of the pair formation described by the iterative process used to solve (17) and (18) leads in most of the cases to a zero solution for $W(\omega)$. The vertex effects have two contrary consequences: they largely complicate the iterative process, because they produce a narrowing of the splitting between the central electronic structures, but this also implies subsequent population of states at the proximity of E_F, this fact being decisive for obtaining superconductivity for some values of the band parameters.

In addition, it is worthwile to say that when one finds a point on the space of the band parameters where superconductivity is possible, the process for obtaining solutions in near points presents a great computational simplification, since one can use this solution of the γ and W functions as the zero iteration for the new points where one looks for superconductivity. This largely decreases the number of iterations needed to obtain convergent and nonzero solutions for $W(\omega)$ in these new points.

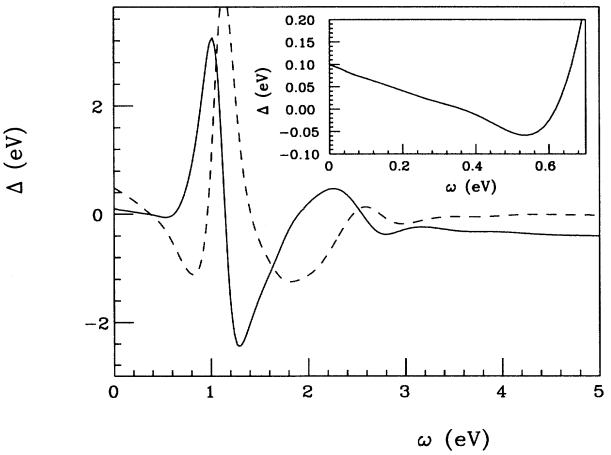

FIG. 7. Real (solid line) and imaginary (dashed line) parts of the superconducting gap function considering vertex effects. Here, $n = 0.5$ (half occupation), U=9 eV, $y = 0.3-0.15i$ eV, and $\Omega_1 = 1.25 - 0.31i$ eV; $\lambda = 0.15$ eV and $\Lambda = 0.075$ eV. Inset: detail of the real part of the gap near the origin.

Transition temperature

In the superconducting region, we also have determined and analyzed the transition temperature. We are now interested in the evolution and tendency of the gap function and the critical temperature when varying the band and potential parameters (λ, Λ, U, n, Ω_1, Ω_2, y),

and for the sake of the simplicity, we will focus on the region of large bandwidths. The critical temperature is found by considering in the integrand of (17) and (18) that $W(\omega') \ll \omega' Z(\omega')$ for all ω' and thus, for $T \to T_c$,

$$W(\omega) = \int_{-\infty}^{\infty} A(\omega,\omega')W(\omega')d\omega' \ , \tag{22}$$

$$A(\omega,\omega') = K_W(\omega,\omega') \times \mathrm{Im} \int_{-\infty}^{\infty} dx \frac{-N(x)}{\omega'^2 Z(\omega')^2 - x^2} \ , \tag{23}$$

$$S(\omega) = -\int_{-\infty}^{\infty} K_S(\omega,\omega')d\omega' \times \mathrm{Im} \int_{-\infty}^{\infty} \frac{N(x)}{\omega' Z(\omega') - x} dx, \tag{24}$$

with $K_W(\omega,\omega')$ and $K_S(\omega,\omega')$ being the same as in (19) and (20), respectively. We have also solved (22-24) self-consistently, fixing a T_c and determining the U value for which there is a convergent result of $\Delta(\omega)$. This calculation, see Fig. 8, allows us to give $U = U(T_c, \Omega, \lambda, \Lambda, n)$, and, therefore, $T_c = T_c(U, \Omega, \lambda, \Lambda, n)$. In this figure, we show the evolution of T_c versus U for different values of the splitting λ and of the width Λ of the Lorentzian DOS, using Eqs. (22–24). Several points can be noted. (i) When comparing with the results obtained with the full RPA effective interaction given in Ref. 3, one observes that the necessary U to have a given T_c is now much lower: the antiparallel-spin effective interaction is more efficient for coupling the fermions because with a value of U around 5 times smaller than in the RPA case we obtain a similar T_c. (ii) With this plot, it is not clear whether a minimum U energy is required to give rise to superconductivity or not. (iii) T_c is very sensitive to variations of the band parameters λ and Λ. The latter is reasonable, as suggested by the strong variation of T_c with the hydrostatic pressure, which is an external agent that modifies the DOS near the Fermi level.

The dependence of T_c on the band parameters has been extensively studied in this work (see Figs. 8 and 9). In Fig. 8(a) is shown the variation of T_c vs U for different values of λ, the semisplitting of the structures at both sides of E_F, fixing their half-widths Λ. We find that for a given value of U, T_c is enhanced as one lowers λ, and, therefore, as the DOS near E_F increases. This behavior holds until a quite low value of λ is reached. Figure 8(b) shows the evolution of T_c vs U with variations of Λ for a fixed value of λ. The result is, in a sense, surprising. For any fixed U value, T_c rises when increasing Λ until $\Lambda \sim \lambda$ [see curves A, B, C of Fig. 8(b)]. For larger values of Λ (i.e., for $\Lambda > \lambda$), the behavior is opposite: T_c lowers when Λ increases (see curves D, E, F). This implies that there exists a value of Λ that is optimum (with T_c maximum) for each value of λ.

To explain this behavior of T_c, we consider that a larger DOS in the energy interval where the gap $\Delta(\omega)$ is positive (see Fig. 6), reinforces the superconductivity, inducing a higher T_c. In opposition, a higher DOS in the energy

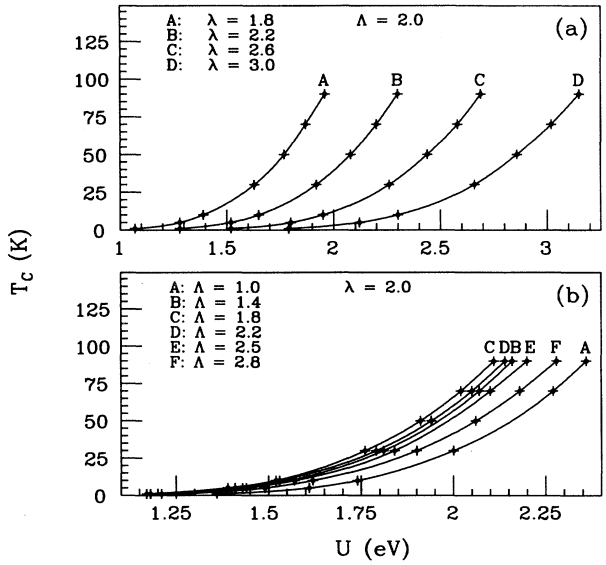

FIG. 8. Evolution of T_c versus the U energy for various values of λ (a) and Λ (b). In all cases $\Omega_1 = 1.25 - 0.31i$ and $y = 0.3 - 0.15i$.

interval where the gap is negative, implies a decrease of the transition temperature. This is also coherent with the fact that the potential is attractive for small energies, and repulsive for energies larger than a given value. When varying λ with Λ fixed, the evolution of the DOS is such that for decreasing λ, the DOS is enlarged in the interval between the two Lorentzians, that is, in the interval where the gap is positive. Thus, the behavior of Fig. 8(a) is reasonable given that T_c augments when decreasing λ, because in this case the DOS in the interval corresponding to positive values of the gap always increases. The evolution of the critical temperature shown

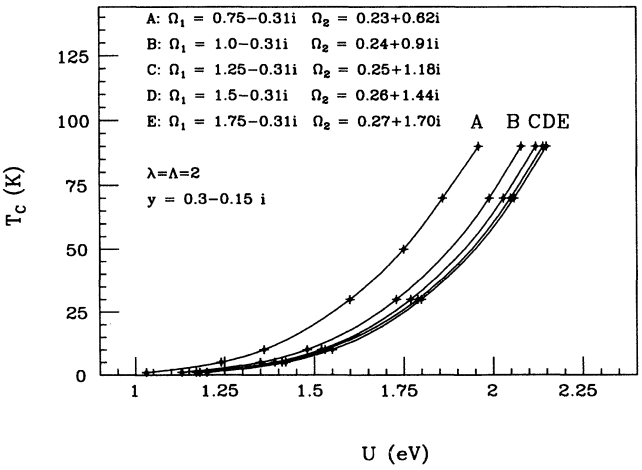

FIG. 9. T_c vs U for different values of $\mathrm{Re}\Omega_1$. In all cases $\lambda = \Lambda = 2$, $y = 0.3 - 0.15i$.

in Fig. 8(b) is somewhat more complex, but is also reasonable. For increasing values of Λ up to $\Lambda \sim \lambda$, the T_c rises because the DOS in the interval where the gap is positive grows faster than in the region where the gap is negative (region of larger energies). The total balance is an increase of T_c. However, when $\Lambda > \lambda$, there is a less important growth of the DOS in the energy interval with positive gap and a simultaneous larger growth in the interval where $\Delta(\omega)$ is negative. Therefore, the balance in this case is a decrease of T_c for increasing values of Λ. On the other hand, the fact that the Λ variations modify the critical temperature after a balance of two opposite simultaneous effects is reflected in the fact that T_c is much more sensitive to variations of λ (which imply the increase of the DOS only in the favorable region) rather than to variations of Λ, as may be seen in Fig. 8.

As we have said above, the poles $\hbar\Omega_1$ and $\hbar\Omega_2$ have the physical meaning of energies of the effective bosons intermediating in the fermion-fermion interaction. Therefore, it is interesting to know the evolution of the superconductivity as a function of these energies. Recall that, according to expression (11), Ω_1 and Ω_2 are related to each other. If one considers Ω_1 as the independent parameter, one sees that an increase of $\mathrm{Re}\Omega_1$ hardly changes $\mathrm{Re}\Omega_2$, but produces an appreciable increase in $\mathrm{Im}\Omega_2$. In Fig. 6, the dependence of the gap on $\mathrm{Re}\Omega_1$ is shown. The effect of lowering $\mathrm{Re}\Omega_1$ is to diminish the frequency range where the gap is positive, while it hardly modifies the magnitude of the gap near the origin, except when one appreciably decreases $\mathrm{Re}\Omega_1$. Of course, the gap should disappear below a certain width of the coupling region of the potential. The large-frequency part of the gap is what more appreciably changes, diminishing when $\mathrm{Re}\Omega_1$ decreases. In Fig. 9 is shown the dependence of T_c on U for various values of $\mathrm{Re}\Omega_1$ (and, therefore, also of $\mathrm{Im}\Omega_2$). One sees that for a given U, the critical temperature varies slightly, perhaps more appreciably when T_c is larger. However, the tendency is that T_c rises when $\mathrm{Re}\Omega_1$ decreases. This might be surprising because it means that T_c is larger when the frequency range where the potential is negative is smaller. However, there are several reasons that may enhance the critical temperature in this case.

(i) When $\mathrm{Re}\Omega_1$ is smaller, the value of the potential at the origin is more negative (attractive), as shown in the inset of Fig. 6.

(ii) The negative part of the gap lowers very appreciably when $\mathrm{Re}\Omega_1$ decreases, while the positive part of the gap decreases but more slowly, at least until a certain value of $\mathrm{Re}\Omega_1$ is exceeded.

(iii) Considering the temporal Fourier transformation of the potential expressed in Eq. (7), one sees that the real part of each pole Ω_k gives the frequency of the corresponding oscillating potential, while the imaginary part is the damping rate of this oscillator. Then, for each pole, the corresponding effective interaction term is attractive during a time interval $\pi/\mathrm{Re}\Omega_k$, and this would yield a larger T_c for smaller $\mathrm{Re}\Omega_k$. However, this does not seem to be a useful argument since on the other half period the potential is repulsive so it would lead to the contrary conclusion. On the other hand, $\mathrm{Re}\hbar\Omega_k$ can be interpreted as the energy of the intermediating boson which produces the pair potential. In phononic superconductors in which the electronic DOS is considered as constant in the proximity of E_F, an increase of the Debye frequency (which could be considered equivalent to $\mathrm{Re}\Omega_k$ in our model) implies an augment of T_c. Therefore, it seems clear that the increase of the exchanged boson energy is what implies a growth of T_c in these cases. In the spin-fluctuation pair potential as studied in our case, the T_c dependence on $\mathrm{Re}\Omega_k$ presents an additional complexity, because the normal-state electronic DOS is not constant, but presents the PR characteristic structures near E_F. This may even invert the tendency of T_c when varying Ω_k. The nonconstancy of the electronic DOS has been quoted as a determinant characteristic in other families of theories for explaining SCS superconductivities.[16] In our model, the importance of the DOS effects is manifested, for instance, by comparing the larger dependence of T_c on λ and Λ (shown in Fig. 8), with respect to the smaller dependence of T_c on $\mathrm{Re}\Omega_k$ (see Fig. 9). If the DOS effects on the Eliashberg equations were neglected, as in Ref. 3, a similar curve of T_c vs U for various Ω_k values would show the expected increase of T_c when enlarging $\mathrm{Re}\Omega_k$.

(iv) We also note that increases of $\mathrm{Re}\Omega_1$ imply larger values of $\mathrm{Im}\Omega_2$, since they are related by Expression (11), while $\mathrm{Re}\Omega_2$ remains almost constant (see the values used in Fig. 9). Larger values of $\mathrm{Im}\Omega_2$ also contribute to a lowering of the pairing effects, because then the damping rate of this second oscillator is larger, and this also contributes to the decrease of T_c. However, it should be noted that the second oscillator has less influence because, for reasonable values of the other parameters, the imaginary part of its pole Ω_2 is larger than that of Ω_1, so the damping of this oscillator is also larger.

(v) We finally remark that it should be taken into account that all the parameters defining the DOS and the pair potential are related. Fixed U and the band occupation n, a smaller Ω_k requires smaller values of λ, which imply strong increases on T_c, as shown in Fig. 8. Therefore, the net effect when decreasing $\mathrm{Re}\Omega_k$ is, in fact, an augment of T_c, but rather due to the necessary narrowing of the splitting between the DOS structures close to E_F than to the variation of $\mathrm{Re}\Omega_k$. It should be noted that when one varies a band parameter in the spin-fluctuation scheme, one is indeed switching on several competitive effects, especially when one is looking for a superconducting state, and, therefore, the behavior is very sensitive to changes of the band parameters.

IV. CONCLUSIONS

We have found and analyzed an effective potential between fermions with antiparallel spins with the corresponding terms of the RPA, plus those of the EHLA series. We have obtained a frequency range where this interaction is attractive. Vertex effects are also considered and we have determined that they are important for small values of the bandwidths (splitting between the two resonances at both sides of E_F, and their respec-

tive widths). We have introduced this effective potential into the Eliashberg-like equations and found that they yield solutions compatible with superconductivity. The parameter compatibility is full in some cases when we include vertex effects in the pair potential. When one considers the pair potentials without vertex effects, it is possible to obtain superconductivity, but only if one takes the real part of the frequency for some equivalent oscillator smaller than that deduced by means of the expressions arising from the spin-fluctuation theories within the Berk-Schrieffer scheme. We have carried out an extensive analysis of the evolution of T_c with the band parameters and remarked that there are optimum values of the DOS near E_F for obtaining high transition temperatures: they correspond to two Lorentzian curves, where the width and the splitting between them have similar values.

ACKNOWLEDGMENT

We acknowledge financial support from DGICYT Project No. PB93-1249.

[1] A.P. Kampf and J.R. Schrieffer, Phys. Rev. B **41**, 6399 (1990).
[2] A.P. Kampf and J.R. Schrieffer, Phys. Rev. B **42**, 7967 (1990).
[3] F. López-Aguilar, J. Costa-Quintana, and L. Puig-Puig, Phys. Rev. B **48**, 1128 (1993); L. Puig-Puig, F. López-Aguilar, and J. Costa-Quintana, J. Phys. Condens. Matter **6**, 4929 (1994).
[4] J.R. Schrieffer, X.G. Wen, and S.C. Zhang, Phys. Rev. B **39**, 11 663 (1989); T.C. Choy and M.P. Das, *ibid.* **47**, 8942 (1993); P. Monthoux and D.J. Scalapino, Phys. Rev. Lett. **72**, 1874 (1994); Chien-Hua Pao and N.E. Bickers, *ibid.* **72**, 1870 (1994).
[5] P. Monthoux and D. Pines, Phys. Rev. B **47**, 6069 (1993); Y. Bang, K. Quader, E. Abrahams, and P.B. Littlewood, *ibid.* **42**, 4865 (1990).
[6] M.M. Steiner, R.C. Albers, D.J. Scalapino, and L.J. Sham, Phys. Rev. B **43**, 1637 (1991); R.M. Martin, Phys. Rev. Lett. **48**, 362 (1982).
[7] N.F. Berk and J.R. Schrieffer, Phys. Rev. Lett. **17**, 433 (1966).
[8] D.J. Scalapino, E. Loh, and J.E. Hirsch, Phys. Rev. B **35**, 6694 (1987).
[9] N. Bulut, D.J. Scalapino, and S.R. White, Phys. Rev. B **47**, 2742 (1993).
[10] M. Grawosky and L.J. Sham, Phys. Rev. B **29**, 6132 (1984); L.J. Sham, Physica **135B**, 451 (1984); F. Mila and E. Abrahams, Phys. Rev. Lett. **67**, 2379 (1991); P.B. Littlewood and C.M. Varma, Phys. Rev. B **46**, 405 (1992); S. Wermbter, *ibid.* **49**, 6869 (1994); F. Manghi, C. Calandra, and S. Ossicini, Phys. Rev. Lett. **73**, 3129 (1994); J. Igarashi, P. Unger, K. Hirai, and P. Fulde, Phys. Rev. B **49**, 16 181 (1994); C. Calandra and F. Manghi, *ibid.* **50**, 2061 (1994).
[11] P.E. Lammert, D.S. Rokhsar, S. Chakravarty, S. Kivelson, and M.I. Salkola, Phys. Rev. Lett. **74**, 996 (1995).
[12] G. Varelogiannis, Phys. Rev. B **50**, 15 974 (1994).
[13] A.B. Migdal, Zh. Eksp. Teor. Fiz. **34**, 1438 (1958) [Sov. Phys. JETP **7**, 996 (1958)]; G.D. Mahan, *Many Particle Physics* (Plenum Press, New York, 1990), p. 828.
[14] P.B. Littlewood, in *Correlated Electron Systems*, edited by V.J. Emery (World Scientific, Singapore, 1993).
[15] D.J. Scalapino, in *Superconductivity*, edited by R.D. Parks (Dekker, New York, 1969), Vol. 1, p. 449.
[16] E. Dagotto, A. Nazarenko, and A. Moreo Phys. Rev. Lett. **74**, 310 (1995); K. Gofron *et al.*, *ibid.* **73**, 3302 (1994); D.M. Newns *et al.*, *ibid.* **69**, 1264 (1992).